



Intervention of resource allocation strategies on spatial spread of epidemicsKebo Zhang,¹ Yuexing Han ,^{1,2,*} Min Gou,¹ and Bing Wang ^{1,†}¹*School of Computer Engineering and Science, Shanghai University, 99 Shangda Road, Shanghai 200444, People's Republic of China*²*Zhejiang Laboratory, Hangzhou 311100, China*

(Received 1 September 2021; accepted 31 March 2022; published 28 June 2022)

Medical resources are crucial in mitigating epidemics, especially during pandemics such as the ongoing COVID-19. Thereby, reasonable resource deployment inevitably plays a significant role in suppressing the epidemic under limited resources. When an epidemic breaks out, people can produce resources for self-protection or donate resources to help others for treatment. That is, the exchange of resources also affects the transmission between individuals, thus, altering the epidemic dynamics. To understand factors on resource deployment and the interplay between resource and transmission we construct a metapopulation network model with resource allocation. Our results indicate actively or promptly donating resources is not helpful to suppress the epidemic under both homogeneous population distribution and heterogeneous population distribution. Besides, strengthening the speed of resources production can significantly increase the recovery rate so that they reduce the final outbreak size. These results may provide policy guidance toward epidemic containment.

DOI: [10.1103/PhysRevE.105.064308](https://doi.org/10.1103/PhysRevE.105.064308)**I. INTRODUCTION**

Curbing the spread of epidemics is vital to human society today. During the past decades, humanity has experienced several major pandemics, such as severe acute respiratory syndrome (SARS) in 2003 [1–3], Middle East respiratory syndrome (MERS) [4,5], West African Ebola [6–8], and so on. Currently, the ongoing novel corona virus disease (COVID-19) has diffused to almost every country in a short period of time, which has been characterized as a public health emergency of international concern (PHEIC) by the World Health Organization [9–12]. With the increase of new infected cases, there is an enormous demand for medical resources, such as ventilators, medical equipment, medicine, and so on [13]. Some countries (regions or cities) have excessively consumed medical resources because of curing massive infected cases, leading to healthcare systems being overwhelmed [14,15]. Importantly, medical resources play a crucial role in curbing the epidemic, and greatly affect the spread process. However, faced with the outbreak of the epidemic, it is necessary that countries (regions or cities) produce medical resources for self-protection, as well as contributing (receiving) resources to (from) others cannot be ignored. Thus, there is an urgent need to better deploy limited medical resources to restrain the spread of epidemic.

The studies about the effects of medical resources on suppressing epidemic through network science are widespread [16–20]. Worby *et al.* [21] studied the distribution of protective resource, namely face masks, during the COVID-19 pandemic, and found that random distribution of masks is not optimal, and prioritized coverage of the elderly or

asymptomatic carriers is more effective. In addition, different from the protective resource, some studies have investigated how best to allocate limited curative resources for curing infected cases based on single layer networks [22,23]. Further, considering different effects such as epidemic spreading and information diffusion, a number of studies have investigated the coevolution dynamics coupling resource allocation with multilayer networks [24–27]. However, these studies are mainly carried out via contact networks in which nodes represent individuals and links denote the contacts between individuals. Nowadays, due to frequent spatial activities of humans and convenient traffic such as airline networks, epidemics especially COVID-19 can rapidly diffuse through the migration of population. Therefore, the deployment of curative resources for treating a large number of infected cases to curb epidemics between locations is crucially important.

Metapopulation network model can be well used to investigate the spatial spread of epidemic due to the mobility of individuals [28–33]. In this framework, nodes represent subpopulations (e.g., regions, cities, or countries), while links represent the migration routes between subpopulations. The infection occurs by the interaction of individuals within a subpopulation and the diffusion corresponds to their migration along the links between subpopulations, which is called reaction-diffusion (RD) process [31,34,35]. Some studies have explored the effects such as mobility rate and nonuniform intervention for suppressing epidemic [28,36,37], whereas factors such as medical resources for treatment inevitably playing the uttermost role in suppressing epidemic have been ignored. With the outbreak of COVID-19 in Wuhan, China, the government promptly deployed medical resources for curing vast infected individuals from other cities to Wuhan and consequently controlled the epidemic. Hence, when facing an epidemic, deploying limited resources reasonably to locations plays a fundamental role in suppressing the epidemic.

*han_yx@i.shu.edu.cn

†bingbignwang@shu.edu.cn

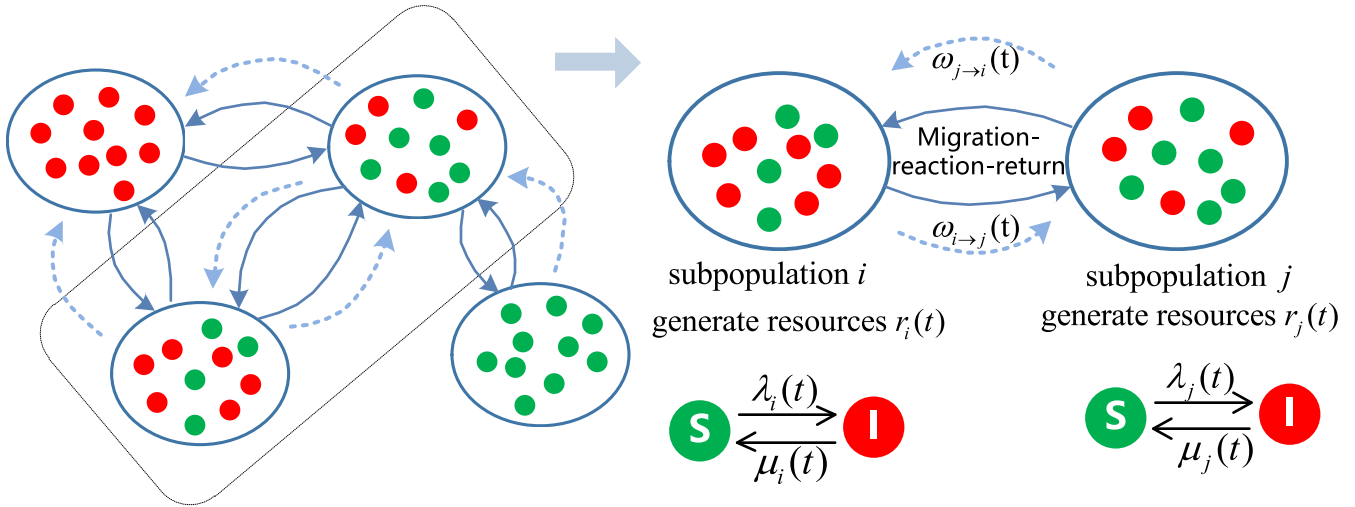


FIG. 1. Schematic diagram of the migration-interaction-return (MIR) metapopulation network model with resource allocation. First, local individuals may move to neighboring subpopulations along the links (solid arrow). Once individuals moved, they will react in a well-mixed way according to the SIS model. Susceptible individuals in subpopulation i get infected at rate $\lambda_i(t)$ while infected individuals get recovered at rate $\mu_i(t)$. The parameters $\lambda_i(t)$ and $\mu_i(t)$ dynamically change with time due to the exchange of resources between subpopulation i and its neighbors, $\omega_{i \rightarrow j}$ or $\omega_{j \rightarrow i}$ (dotted arrow). After reaction, they return to their resident subpopulations and the next time step starts.

Generally, infected individuals consume medical resources for treatment, while susceptible individuals are responsible for producing resources to support infected ones. So, subpopulations which contain susceptible individuals will generate resources to help each other to restrain the epidemic. Without a doubt, after exchange of resources between subpopulations, the infection rate and the recovery rate will alter. Naturally, a subpopulation becomes risky to be infected after donation, while it is helpful for treatment when holding more resources. Thus, we can formulate the epidemiological process with the resource donation process. In other words, one subpopulation gets a higher infection rate when it donates resources to others. Instead, it gets a higher recover rate when holding more resources, i.e., it produces or receives more resources. In short, by producing and donating resources to infected subpopulations, the epidemic process coevolves with the resource donation dynamics.

Here, we construct a metapopulation network model with Migration-Interaction-Return (MIR) to investigate the coevolution dynamics of epidemic spreading and resource allocation (Fig. 1). Specifically, we model the spatial spreading of the epidemic through the reaction-diffusion process based on the classical susceptible-infected-susceptible (SIS) [38] model. Besides, the microscopic Markov chain theory is applied to derive the epidemic threshold, and Monte Carlo (MC) simulation is used to verify the accuracy with the Markov equations.

II. MODEL DESCRIPTION

A. Metapopulation network model with resource allocation

Faced with the outbreak of the epidemic, each subpopulation can generate resources for battle against the disease at each time step. Intuitively, infected individuals consume medical resources, while susceptible ones are responsible for producing curative resources to treat infected ones. So we

reasonably assume that the amount of resources produced by one subpopulation is positively correlated to its current proportion of susceptible individuals. Accordingly, we define the resources availability $r_i(t)$ of subpopulation i at time t as follows:

$$r_i(t) = \theta[1 - \rho_i(t)], \quad (1)$$

where $\rho_i(t)$ is the ratio of infected individuals in subpopulation i at time t , and $\theta (\geq 1)$ is the coefficient denoted as the rate of the resources' arrival. Higher θ means a faster speed of resource producing.

When an epidemic breaks out, subpopulation i perceives the threat intuitively from neighbors. So, to quantify the response strength of a subpopulation to the disease, a parameter $\alpha_0 \in [0, 1]$ denoting awareness is introduced, and a higher α_0 means that fewer resources will be donated. Usually, the more infected individuals around a subpopulation, the more resources are supposed to be donated to them. Hence, we assume that the donation willingness of subpopulation i increases with the ratio of infected individuals around it. In addition, considering the reality of self-protection, subpopulation i will not contribute any resources if its current available resources is below a threshold r_0 . Thus, we define donation willingness of subpopulation i at time t $q_i(t)$ as follows:

$$q_i(t) = q_0[1 - \alpha_i(t)] \frac{1}{1 + e^{-\beta[m_i(t) - \eta]}}, \quad (2)$$

where

$$\alpha_i(t) = \begin{cases} \alpha_0, & \text{if } r_i(t) \geq r_0, \\ 1, & \text{else} \end{cases}$$

denotes the donation awareness of subpopulation i at time t . Besides, q_0 is a basic donation factor, $m_i(t)$ is the ratio of infected individuals in the neighboring set of subpopulation i , $V(i)$, at time t , and the coefficient $\beta (\geq 0)$ represents the

donation sensitivity. The sigmoid function $\frac{1}{1+e^{-\beta(m_i(t)-\eta)}}$, which is plotted as shown in Fig. 9, Appendix A 3, on the right side of Eq. (2) represents donation sensitivity to the infection, where $\eta \in [0, 1]$ controls the horizontal shift of the function, and a higher η induces a lower initial value of $q_i(t)$. A smaller β means that the subpopulation is more sensitive to degree of infection around the neighbors of set $V(i)$. Besides, the smaller β indicates that donation willingness gets a higher initial value and increases steadily with $m_i(t)$ in a less slope. That is, how many resources will be donated depends on the infected degree around the subpopulation i , denoted as $m_i(t)$ and expressed as follows:

$$m_i(t) = \frac{\sum_{k \in V(i)} I_k(t)}{\sum_{k \in V(i)} N_k}, \quad (3)$$

where $\sum_{k \in V(i)} N_k$ and $\sum_{k \in V(i)} I_k(t)$ are the total population and the total of infected population in the neighboring set of subpopulation i , $V(i)$.

With the emergence of infected individuals in neighbors of subpopulation i , it would release part of its resources to help neighbors curb the disease. Additionally, we assume that not all the subpopulations receive resources, only those with infection scale higher than some value will receive resources, and the amount of resources that a subpopulation receives is proportional to its infection degree, that is, a subpopulation j with infection rate higher than i_0 would receive sources. Accordingly, the resource flow that subpopulation i releases to one neighbor j at time t can be denoted as follows:

$$\omega_{i \rightarrow j}(t) = \begin{cases} r_i(t)q_i(t) \frac{I_j(t)}{\sum_{k \in V(i)} I_k(t)}, & \text{if } I_j(t)/N_j \geq i_0, \\ 0, & \text{else,} \end{cases} \quad (4)$$

where i_0 is the threshold for infection ratio, $V(i)$ is the neighboring set of i , $\sum_{k \in V(i)} I_k(t)$ is the total infected population in set $V(i)$, N_j and $I_j(t)$ are the number of population and that of the infected population of j , respectively, and $q_i(t)$ is donation willingness of subpopulation i at time t .

When infected individuals emerge around subpopulation i , it intends to donate resources to neighboring subpopulations to suppress diseases, while protecting itself from infection. However, donating resources may lead to an increasing risk of infection due to the lack of sufficient awareness for self-protection. We connect the infectivity within a subpopulation with the donation willingness for the resources. Hence, we consider a modified infection rate after donating resources at time t $\lambda_i(t)$ with a penalty coefficient $c \in [1, 3]$, and $\lambda_i(t)$ is

expressed as

$$\lambda_i(t) = q_i(t)c\lambda + [1 - q_i(t)]\lambda, \quad (5)$$

where λ is the basic infection rate, and $q_i(t)$ is the donation willingness of subpopulation i at time t as mentioned above. Apparently, the infection rate recovers a constant λ if $c = 1$, i.e., there is no impact when donating resources to others. On the contrary, if $c > 1$, then there is a relatively higher infection rate in subpopulation i when donating resources. The above definition means that the infection rate usually varies from subpopulation to subpopulation with time.

In general, a subpopulation can generate resources by itself or receive them from others. So, the resources that a subpopulation i holds at time t are expressed as follows:

$$\omega_i(t) = r_i(t)[1 - q_i(t)] + \sum_{j \in V(i)} \omega_{j \rightarrow i}(t), \quad (6)$$

where the first term denotes its remaining resources after donation and the second denotes the resources received from others. Generally, a subpopulation has a higher recovery rate if it holds more resources. So, the recovery rate of subpopulation i at time t , $\mu_i(t)$, can be defined as

$$\mu_i(t) = 1 - (1 - \mu)^{1 + \varepsilon \omega_i(t)}, \quad (7)$$

where μ is the basic recovery rate, and $\varepsilon \in [0, 1]$ is resource utilization rate. Apparently, we can see that recovery rate of subpopulation i keeps the constant value μ if $\varepsilon = 0$ or without resources; otherwise, the recovery rate will be affected in a limited scope with further growth resources $\omega_i(t)$. Similarly, the recovery rate generally varies from subpopulation to subpopulation with time.

B. Microscopic Markov chain method and threshold analysis

Based on the above model description, we construct a metapopulation network model composed a total of N subpopulations. Each subpopulation i has a number of n_i individuals, $\forall i = 1, 2, \dots, N$. At the migration stage, an individual leaves its resident subpopulation i with probability p , and migrates to one of its neighboring subpopulations j in terms of the transition matrix R , whose entries are $R_{ij} = \frac{W_{ij}}{\sum_{j=1}^N W_{ij}}$, where W_{ij} denotes the weight between subpopulation i and j . Then, once individuals have moved, they interact in a well-mixed pattern in each subpopulation i and change their epidemic status in terms of current infection rate $\lambda_i(t)$ and recovery rate $\mu_i(t)$ at time t based on SIS model. Finally, they return to their resident subpopulation and next time step starts. Here, we derive the epidemic threshold with $r_0 = 0.0$ and $i_0 = 0.0$ for simplicity. In the following, we find that there are no obvious impacts of them on the final results with simulations (see Appendix A 1).

There are N variables $\rho_i(t)$ denoting the ratio of infected individuals associated with subpopulation i at time t . The time evolution of $\rho_i(t)$ can be written as follows:

$$\rho_i(t + 1) = \rho_i(t) \left\{ (1 - p)[1 - \mu_i(t)] + p \sum_{j=1}^N R_{ij}[1 - \mu_j(t)] \right\} + [1 - \rho_i(t)]\Gamma_i(t), \quad (8)$$

where the first term on the right side is the fraction of infected individuals who do not recover. The infected individuals are those who remain in subpopulation i and those who migrate to neighboring subpopulations and then return back to subpopulation i . The second term on the right side accounts for the ratio of susceptible individuals associated with subpopulation i that are infected at time t . In this second term, $\Gamma_i(t)$ denotes the probability that susceptible individuals associated with subpopulation i become infected at time t , and reads

$$\Gamma_i(t) = (1-p)P_i(t) + p \sum_{j=1}^N R_{ij}P_j(t), \quad (9)$$

where the first term on the right side is the probability that susceptible individuals, who do not move, get infected in the resident subpopulation i at time t , and the second term denotes the probability that individuals get infected when migrating to any neighboring subpopulation. And $P_i(t)$ is denoted as

$$P_i(t) = 1 - \prod_{j=1}^N [1 - \lambda_i(t)\rho_j(t)]^{n_{j \rightarrow i}}, \quad (10)$$

where $n_{j \rightarrow i}$ denotes the population flux moving from subpopulation j to subpopulation i , and reads

$$n_{j \rightarrow i} = \delta_{ij}(1-p)n_i + pR_{ji}n_j, \quad (11)$$

with $\delta_{ij} = 1$ if $i = j$ and otherwise $\delta_{ij} = 0$.

$$\Gamma_i = \lambda \sum_{j=1}^N \left\{ (1-p)^2 \delta_{ij} n_j + p(1-p) R_{ji} n_j + p(1-p) \theta \left[\frac{q_0(1-\alpha_0)}{1+e^{\eta\beta}} (c-1) + 1 \right] R_{ij} n_j \right\} \varepsilon_j^*, \quad (14)$$

and we define

$$\mathbf{M}_{ij} = (1-p)^2 \delta_{ij} n_j + p(1-p) R_{ji} n_j + p(1-p) \theta \left[\frac{q_0(1-\alpha_0)}{1+e^{\eta\beta}} (c-1) + 1 \right] R_{ij} n_j + p^2 \theta \left[\frac{q_0(1-\alpha_0)}{1+e^{\eta\beta}} (c-1) + 1 \right] (RR^T)_{ij} n_j. \quad (15)$$

Accordingly, we derive the epidemic threshold λ_c as follows:

$$\lambda_c = \frac{T}{\Lambda_{\max}(\mathbf{M})}, \quad (16)$$

where $\Lambda_{\max}(\mathbf{M})$ is the maximum eigenvalue of the matrix \mathbf{M} . Unfortunately, the detailed expression for the maximum eigenvalue of the matrix \mathbf{M} is difficult to obtain. Nevertheless, we can obtain the epidemic threshold by numerical iteration.

III. SIMULATION RESULTS

To understand the coevolution of the epidemic dynamics with resources, we systematically explore the impacts of resource donation, such as the donation awareness α_0 , the donation sensitivity β , and the rate of the resources' arrival θ . We have performed an extensive set of stochastic simulations on the scale-free (SF) networks with 1000 subpopulations, whose average degree is 6.9. The edge weights between subpopulations are uniformly distributed within the range of [1, 50]. Two types of population distributions, i.e., homogeneous distribution (HOD) and heterogeneous distribution (HED), are considered. Under the HOD, each subpopulation equally contains 100 individuals; under the HED, each subpopulation

To analyze the steady state of the dynamics when $t \rightarrow \infty$, namely, $\rho_i(t+1) = \rho_i(t) = \rho_i$, we can simplify Eq. (8) as

$$[1 - (1-p)(1-\mu_i) - p \sum_{j=1}^N R_{ij}(1-\mu_j)] \rho_i = (1-\rho_i) \Gamma_i, \quad (12)$$

where ρ_i is the steady density of infected individuals associated to subpopulation i .

When close to the critical point, let us denote $\rho_i = \varepsilon_i^* \ll 1$ for any subpopulation i . We estimate $\mu_i = \mu(1 + \varepsilon\omega_i)$ neglecting second- and higher-order terms from Eq. (7), and $\omega_i \approx \theta[1 + \frac{k_i q_0(1-\alpha_0)}{1+e^{\eta\beta}}]$. We denote left side of Eq. (12) as follows:

$$[1 - (1-p)(1-\mu_i) - p \sum_{j=1}^N R_{ij}(1-\mu_j)] \varepsilon_i^* = T \varepsilon_i^*, \quad (13)$$

where $T = 1 - (1-p)\{1 - \mu[1 + \varepsilon\theta(1 + \frac{k_i q_0(1-\alpha_0)}{1+e^{\eta\beta}})]\} - p \sum_{j=1}^N R_{ij}\{1 - \mu[1 + \varepsilon\theta(1 + \frac{k_j q_0(1-\alpha_0)}{1+e^{\eta\beta}})]\}$. On the right side of Eq. (12), we have $P_i(t) \approx \sum_{j=1}^N \lambda_i \rho_j n_{j \rightarrow i}$, $n_{j \rightarrow i} = \delta_{ij}(1-p)n_i + pR_{ji}n_j$, and $\Gamma_i \approx (1-p) \sum_{j=1}^N \lambda_i \rho_j n_{j \rightarrow i} + p \sum_{j=1}^N R_{ij} \sum_{l=1}^N \lambda_j \rho_l n_{l \rightarrow j}$, so

i contains a number of population proportional to the sum of the edge weight, i.e., $\sum_{j=1}^N W_{ij}$. The microscopic Markov chain starts by infecting a small fraction of individuals as seeds in each subpopulation. Without loss of generality, 0.1% of individuals is set to be infected initially. Correspondingly, the same initial condition is applied to the Monte Carlo simulations, so each individual is set to be infected with probability 0.001. Considering the general simulations, the parameter η is set at 0.5, and some other parameters are set at default values in Table I.

A. Effects of the resource donation awareness on the epidemic spread

To highlight the effects of each subpopulation's donation awareness α_0 on the epidemic spreading, we set $\beta = 1$ for the general donation sensitivity, and $\theta = 1$ for the normal rate of the resources arrival. Figure 2 shows the final prevalence ρ at steady state versus basic infection rate λ for various values of α_0 under the conditions of HOD and HED, respectively (there is a perfect agreement between the iterations of Markov equations and Monte Carlo (MC) simulations, and the

TABLE I. Involved parameters in the MIR metapopulation network model.

Parameter	Definition	Default value
λ	Basic infection rate	—
μ	Basic recovery rate	0.2
p	Migration probability	0.2
c	Penalty coefficient after donation	2.0
ε	Resource utilization rate	0.6
q_0	Basic donation factor	0.8
θ	The rate of the resources' arrival	—
α_0	Resource donation awareness	—
β	Resource donation sensitivity	—
η	The parameter in the sigmoid function	0.5
r_0	Threshold for donating resources	0.0
i_0	Threshold for receiving resources	0.0

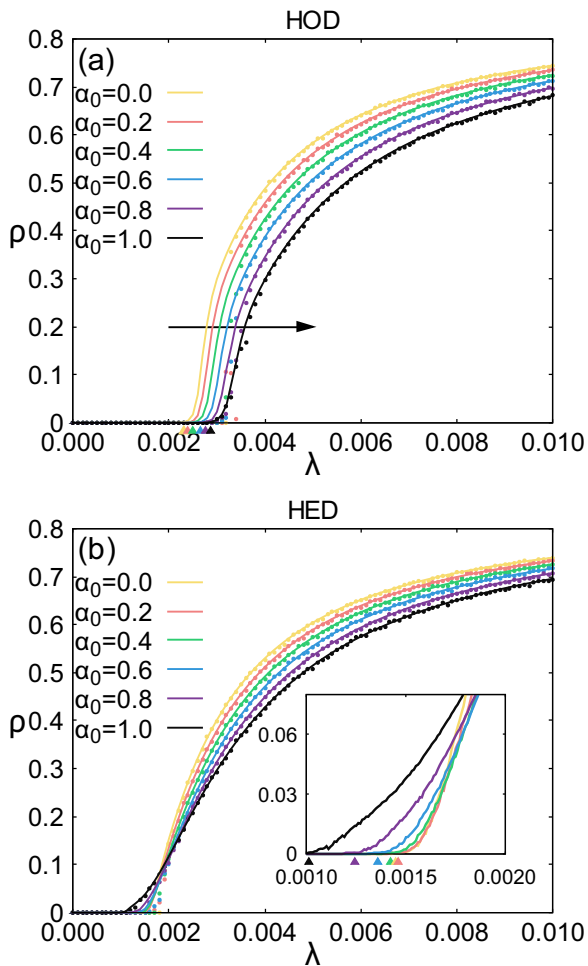


FIG. 2. The final epidemic prevalence ρ versus the basic infection rate λ for various values of the donation awareness α_0 . (a) Homogeneous population distribution (HOD) and (b) heterogeneous population distribution (HED), and the inset shows the detail Markov process as λ between 0.001 and 0.002). The solid curves correspond to the iterations of the Markov equations, whereas the dots represent the results of Monte Carlo (MC) simulations. Each dot is the average over more than 50 MC simulations. The triangles under x axis are the epidemic thresholds by the iteration of the Markov equations. The other parameters β and θ are set as $\beta = 1$ and $\theta = 1$.

similar relationship is no longer emphasized in the following sections). In addition, there is no resource exchange between subpopulations when $\alpha_0=1$, and full donation willingness when $\alpha_0 = 0$. From Fig. 2, the epidemic thresholds under the HOD are overall higher than the HED. Because under the HED some subpopulations with more population have more infected cases initially, the epidemic easily breaks out and quickly spreads out by migration. But under the HOD, the infected cases are uniformly distributed in each subpopulations initially, inducing a slower spreading with a higher epidemic threshold.

For the case of the HOD, we see that lower awareness α_0 or stronger willingness of resource donation among subpopulations would promote the epidemic spread with a reduced epidemic threshold and a larger outbreak size. When an outbreak occurs in a subpopulation, neighboring subpopulations with high donation willingness would donate more resources to it, leading to high infection rates in them. In Fig. 7, Appendix A 2, we find a lower awareness α_0 induces a higher $\langle \lambda \rangle / \langle \mu \rangle$, which supports the results. Thus, it seems that actively donating resources to the infected subpopulation is not helpful to suppress the epidemic.

In contrast, for the case of the HED, we can see that a lower awareness α_0 or a stronger willingness of donation among subpopulations would delay the outbreak of the epidemic with a higher epidemic threshold, but induce a larger final outbreak size. Because under the HED the epidemic would easily break out in subpopulations with more population, a lower awareness indicates that neighboring subpopulations would donate more resources to it, leading to the containment of the epidemic. By grouping the subpopulations according to their population, we find that a higher donation awareness results in a larger ratio of infected individuals in large subpopulations, see Fig. 8, Appendix A 2, for details. But a lower awareness also induces a larger outbreak size as previous situation. It suggests that actively donating resources just delays the outbreak at the early time, but is not helpful to suppress the epidemic while continuously donating resources.

B. Effects of the resource donation sensitivity on the epidemic spread

To understand the impacts of the donation sensitivity β on the epidemic, we set $\alpha_0 = 0$ with no awareness namely full willingness of resource donation, and $\theta = 1$ for the normal speed of resources availability. Figure 3 shows the final prevalence ρ at steady state versus the basic infection rate λ under various values of β . Particularly, the donation willingness is constant, i.e., $\alpha_0 = 0.5$, if $\beta = 0$. From Fig. 3, the epidemic thresholds under the HOD are overall higher than the HED.

Under the condition of the HOD [Fig. 3(a)], we see that higher donation sensitivity (i.e. higher β) can delay the epidemic with a higher epidemic threshold, but induce a larger final break size. This is because a higher β induces a lower initial donation willingness, that is, neighboring subpopulations donate fewer resources when the epidemic breaks out, leading to low infection rates in them. In Fig. 10, Appendix A 3, we testify that a lower β leads to a higher average effective infection rate $\langle \lambda \rangle / \langle \mu \rangle$, which also supports the above results. However, a higher β induces a larger outbreak size because the rapid growth of donation willingness

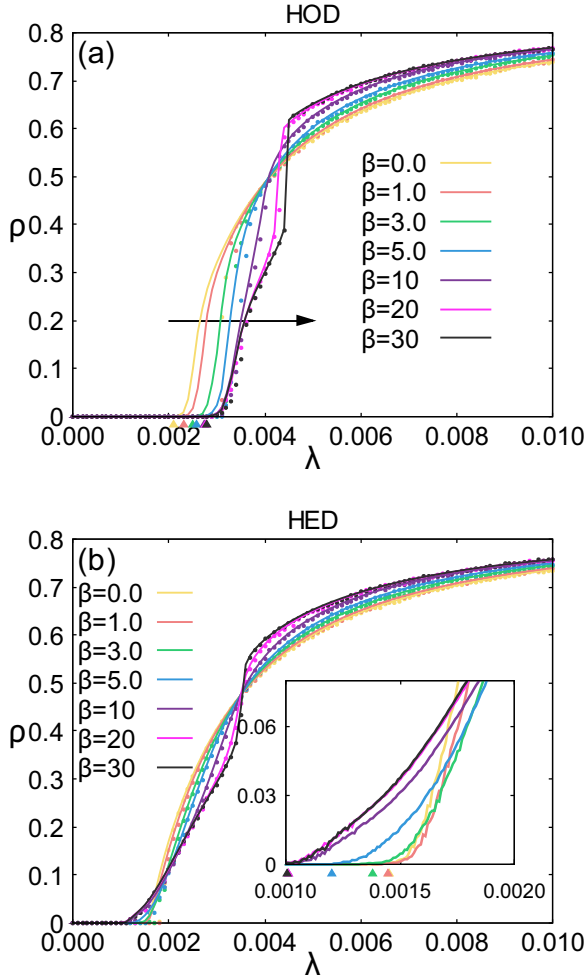


FIG. 3. The final epidemic prevalence ρ versus the basic infection rate for various values of the donation sensitivity β . (a) Homogeneous population distribution (HOD), and (b) Heterogeneous population distribution (HED, and the inset shows the detail Markov process as λ between 0.001 and 0.002). The triangles under x axis are the epidemic thresholds by iteration of the Markov equations. The other parameters α_0 and θ are set as $\alpha_0 = 0$ and $\theta = 1$.

leads to high infection rates in neighboring subpopulations. It seems that donating resources or quickly response to the infected subpopulation would induce high infected scale instead.

Under the condition of the HED [Fig. 3(b)], we can see that a lower donation sensitivity (lower β) can suppress the epidemic outbreak with a higher epidemic threshold and induces a smaller final outbreak size. This is because under the HED the epidemic would easily break out in subpopulations with more population (see Fig. 11, Appendix A 3, for details), who can receive more resources from neighbors to suppress the epidemic due to a higher initial donation willingness with a lower donation sensitivity β , leading to a higher epidemic threshold. However, a higher β also induces a larger final outbreak size. It suggests that donating a big amount of resources earlier just delays the epidemic, and promptly increasing resource donation is also not conducive to reduce final infected scale.

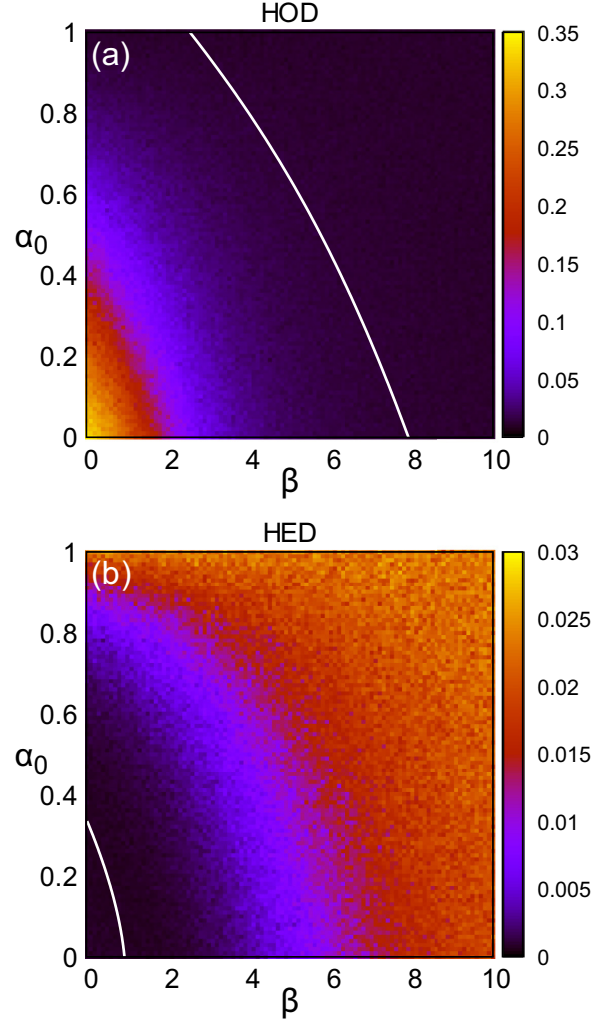


FIG. 4. The epidemic prevalence (color value) as a function of α_0 and β by Monte Carlo (MC) simulations when close to the threshold. (a) Homogeneous population distribution (HOD, $\lambda = 0.00325$) and (b) heterogeneous population distribution (HED, $\lambda = 0.0015$). The white solid lines are corresponding epidemic thresholds of α_0 and β .

C. The coupling effects of donation awareness and donation sensitivity

To elucidate the interplay between the donation awareness α_0 and the donation sensitivity β , we plot the epidemic prevalence under the cases of HED and HOD, respectively, when close to threshold as shown in Fig. 4. For the case of HOD, it shows that high donation awareness and high donation sensitivity can delay the epidemic with a low prevalence, which clearly indicates that donating more resources (lower α_0) may promote the epidemic, and donating resources fewer initially (higher β) can validly suppress the epidemic. Therefore, these results indicate that we need to steadily increase resource donation, avoiding donating a large amount of resources initially without protecting ourselves. Instead, under the case of HED, low donation awareness and low donation sensitivity can suppress the epidemic outbreak, which indicates that we need to immediately donate plenty of resources to infected subpopulations, especially with more population, to rapidly

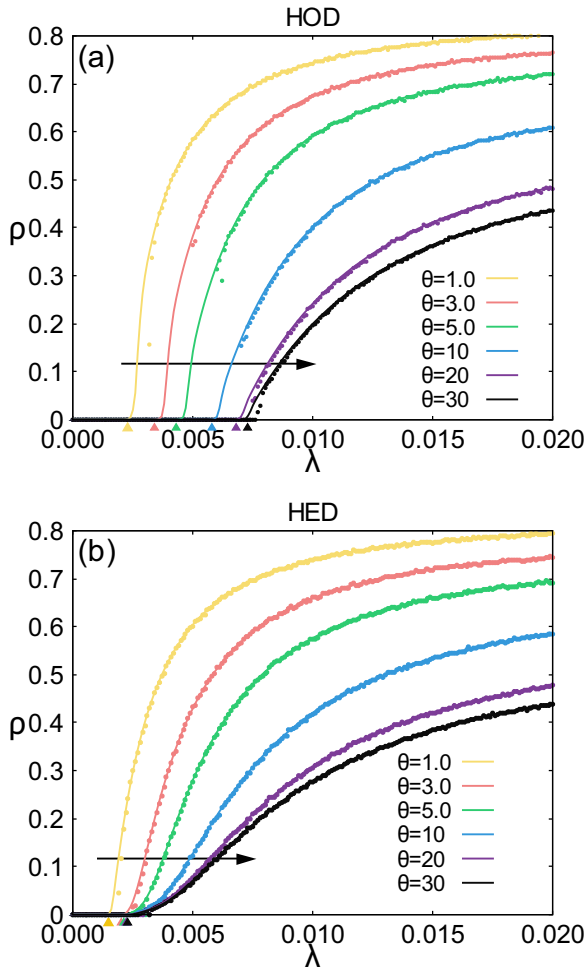


FIG. 5. The final epidemic prevalence ρ versus the basic infection rate λ under various values of the rate of the resources' arrival θ . (a) Homogeneous population distribution (HOD), and (b) Heterogeneous population distribution (HED). The triangles under x axis are the epidemic thresholds by iteration of the Markov equations. The other parameters α_0 and β are set as $\alpha_0 = 0$ and $\beta = 1$.

suppress the epidemic. But promptly increasing the resource donation (higher β) with the growth of outbreak scale is not a valid strategy.

D. Effects of the rate of the resources' arrival on the epidemic spread

Generally, individuals can recover to susceptible state by plenty of curative resources, so the more resources they hold, the higher recovery rate they get. The rate of the resources' arrival θ is the parameter used to measure the speed of resources availability per time step. To interpret the impacts of θ on the epidemic spread, we set $\alpha_0 = 0$ with no awareness namely full willingness of resource donation, and $\beta = 1$ with the general donation sensitivity. Figure 5 shows the final epidemic prevalence ρ versus basic infection rate λ under various values of θ . It can be regarded as a normal speed of resources availability for $\theta = 1$, and higher speed when θ is greater than 1.

From Fig. 5, we see that a higher rate of the resources' arrival θ delays the epidemic with a higher epidemic threshold

and reduces the final outbreak size under the conditions of both the HOD and the HED. This is because subpopulations can produce more resources at each time step so that they hold more resources averagely, which leads to higher recovery rates and lower effective infection rates. This observation is testified in Fig. 12, Appendix A4. In addition, a higher θ can clearly decrease the final epidemic prevalence for all the subpopulations we testified in Fig. 13, Appendix A4. In SF networks with a heterogeneous topology, since hub subpopulations generally have more population with more infected cases initially, the epidemic can easily break out with a lower threshold under the HED.

As a consequence, higher speed of resource production can effectively delay the epidemic spread and reduce final infected ratio regardless of the HOD and the HED, but this effect is finite because the average recovery rate works in a limited scope with further increase of resources. Therefore, properly reinforcing the speed of resources production, such as extending working hours, is necessary for suppressing the epidemic.

IV. DISCUSSIONS AND CONCLUSIONS

Faced with epidemics, especially pandemics such as COVID-19, medical resources undoubtedly play a significant role in suppressing epidemics, so the reasonable deployment about resources become an important issue that we need to further investigate. While most of the advances previously described have been focused on capturing the resource deployment based on contact networks, less attention has been paid on the metapopulation networks. Due to current convenient traffic, the human interactions induce the spatial spreading of epidemics by individuals' movement between regions (or cities, countries), which ignores the role of resource deployment on the so-called metapopulation networks. Recently, Zhu *et al.* [39] have studied the effects of resource allocation on the metapopulation networks, where a subpopulation can allocate one unit resource to neighbors at each time step. In this paper, we consider that subpopulations can generate different amount of resources depending on their resource availability, donating willingness, etc., and donate them to neighboring subpopulations according to their infection degree.

In this work, we construct a metapopulation network model to study the resource deployment on epidemic evolution. The results indicate that properly donating resources can delay the epidemic with a high epidemic threshold under heterogeneous population distribution, but actively or promptly donating resources to the infected subpopulation is not helpful to suppress the epidemic regardless of homogeneous or heterogeneous population distribution. The trade-off between donating resources and self-protection needs to be carefully considered for policy makers when facing an epidemic. Meanwhile, strengthening the speed of resources availability is an effective measure, which can significantly increase average recovery rate and reduce the final outbreak size.

However, our current work inevitably has several limitations. First, we simply consider that the amount of resources generated by one subpopulation is proportional to its ratio of susceptible individuals. However, under heterogeneous population distribution, these subpopulations with more population

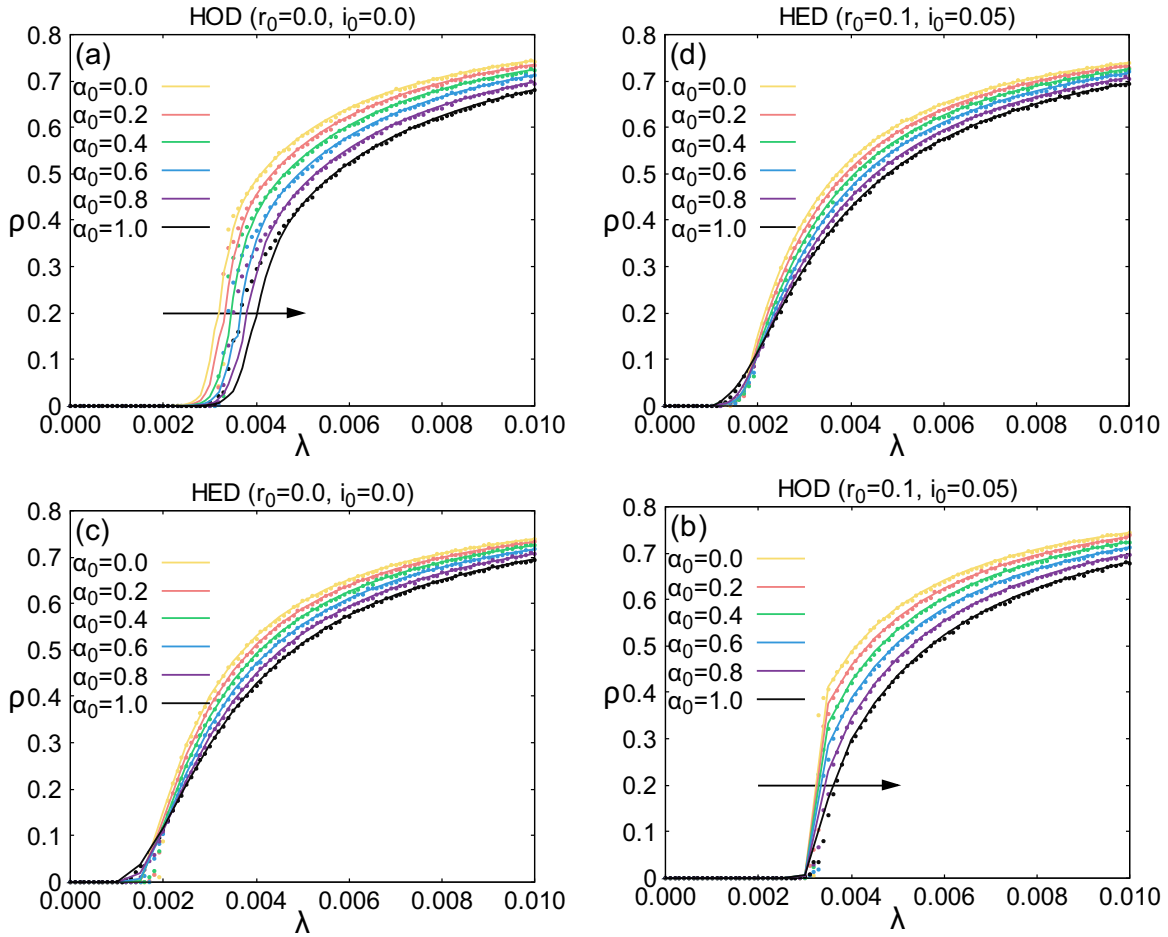


FIG. 6. The final epidemic prevalence ρ for different α_0 under different parameters of r_0 and i_0 . Homogeneous population distribution (HOD), with parameters (a) $r_0 = 0.0, i_0 = 0.0$; (b) $r_0 = 0.1, i_0 = 0.05$. Heterogeneous population distribution (HED), with parameters (c) $r_0 = 0.0, i_0 = 0.0$; (d) $r_0 = 0.1, i_0 = 0.05$. The solid curves correspond to the iterations of the Markov equations, whereas the dots represent the results of Monte Carlo simulations.

tend to generate more resources than those with fewer population, so we can further consider the factor of individuals on resources availability. Besides, we assume resources are produced by each subpopulations itself, but ignore global resources that can be reasonably allocated to each one. The generation and allocation patterns of resources are expected to be further explored and compared in the future.

ACKNOWLEDGMENTS

This research is sponsored by the Natural Science Foundation of Shanghai (Grant No. 20ZR1419000), Key Research Project of Zhejiang Laboratory (Grant No. 2021PE0AC02).

APPENDIX

1. The impacts of parameters r_0 and i_0

To analyze the effects of parameters r_0 and i_0 on the epidemic threshold and the final epidemic prevalence, we have tested different values of i_0 and r_0 under the HOD and HED, as shown in Fig. 6. Under the HOD, with threshold $i_0 = 0.0$ for resource reception, a higher donation awareness α_0 leads to a lower infection rate, which delays the outbreak of the

epidemic initially with a larger epidemic threshold [Fig. 6(a)]. With a lower threshold $i_0 = 0.05$, it is not large enough to trigger the epidemic. Thus, no resource exchange occurs in the network, and we see the same threshold regardless of α_0 . Further, since the epidemic diffuses by a relatively uniform way, a higher i_0 for resource reception has few impacts on the final results. Besides, r_0 also has the similar effects because the resource exchange must meet both i_0 and r_0 . Under the HED, α_0 has no evident influence on the epidemic threshold and the final outbreak sizes [Figs. 6(c) and 6(d)]. This is because under the HED, the epidemic would easily break out in large-scale subpopulations, which is insensitive to the parameter i_0 and r_0 . As a result, r_0 and i_0 have no obvious impacts on the final results under the HOD or HED. Thus, for the simplicity of the derivation of the epidemic threshold, we choose $r_0 = 0.0$ and $i_0 = 0.0$ in our simulations.

2. Effects of the parameter α_0

To further explore the detailed effects of the donation awareness α_0 on the epidemic spreading, we collect the

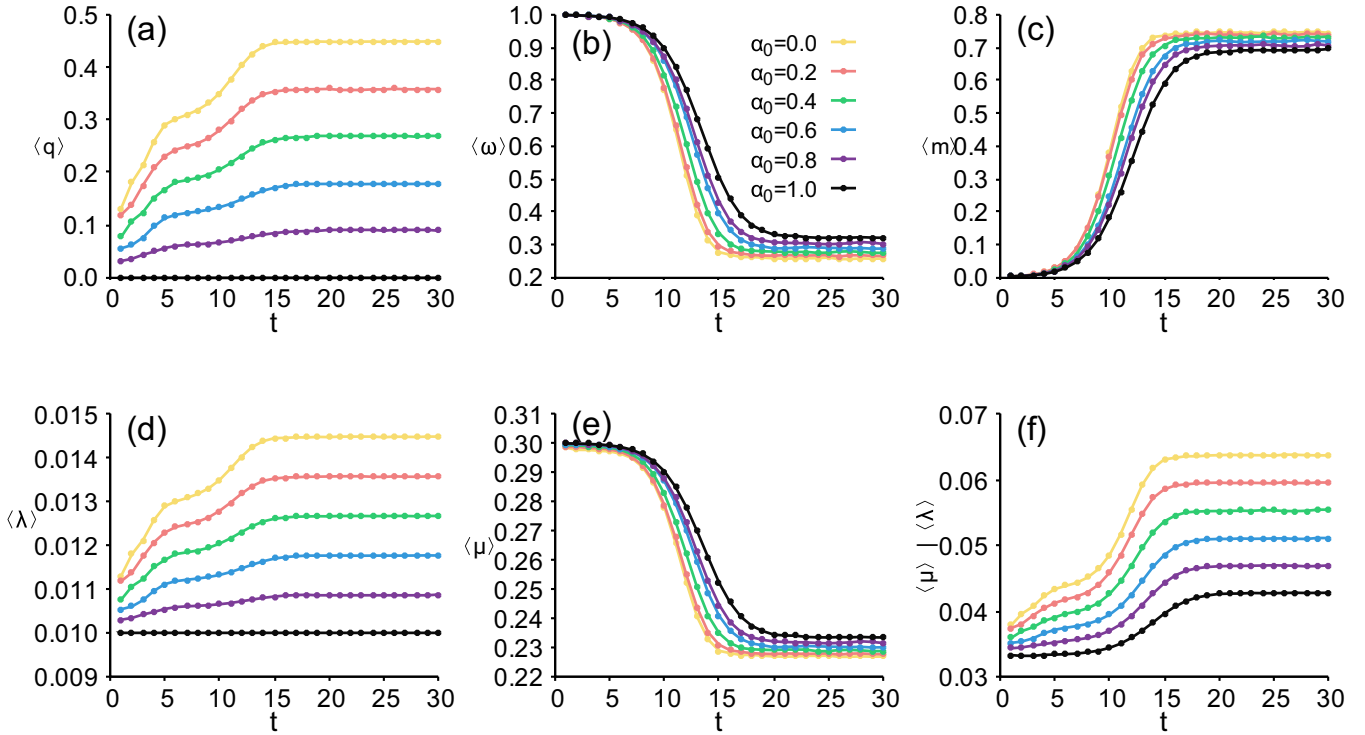


FIG. 7. The time evolution of six properties for various values of α_0 under the HOD. (a) The average donation willingness $\langle q \rangle$; (b) the average holding resources $\langle \omega \rangle$; (c) the average infection ratio of individuals in neighboring subpopulations $\langle m \rangle$; (d) the average infection rate $\langle \lambda \rangle$; (e) the average recover rate $\langle \mu \rangle$; (f) the average effective infection rate $\langle \lambda \rangle / \langle \mu \rangle$. The basic infection rate $\lambda = 0.01$.

statistical properties of the network evolving with time, such as the average donation willingness $\langle q \rangle$, the average holding resources $\langle \omega \rangle$, the average infection ratio of individuals in neighboring subpopulations $\langle m \rangle$, the average infection rate $\langle \lambda \rangle$, the average recover rate $\langle \mu \rangle$, and the average effective infection rate $\langle \lambda \rangle / \langle \mu \rangle$. The initial population is homogeneous (HOD), and the infection rate is $\lambda = 0.01$ (Fig. 7). The average infection ratio of individuals in neighboring subpopulations $\langle m \rangle$ increases promptly with time as shown in Fig. 7(c). The lower α_0 is, the faster it increases. When infected individuals emerge in subpopulations, they will release (receive) resources to (from) neighbors. As we can see from Fig. 7(a), the average donation willingness $\langle q \rangle$ increases with time when $\alpha_0 \neq 1$, and a lower α_0 induces a higher $\langle q \rangle$. However, a higher donation willingness of one subpopulation induces a higher average infection rate $\langle \lambda \rangle$ [Fig. 7(d)]. At the same time, since the increasing of infected individuals induces a lower ability of resources availability, the average holding resources $\langle \omega \rangle$ decrease [Fig. 7(b)]. Meanwhile, since the recovery rate of one subpopulation is positively correlated to its current resources, we see similar trend in Fig. 7(e). Thus, the average effective infection rate $\langle \lambda \rangle / \langle \mu \rangle$ increases with time for each α_0 and a lower α_0 induces a higher $\langle \lambda \rangle / \langle \mu \rangle$ [Fig. 7(f)]. For the HED, to further interpret the role of awareness α_0 near the threshold, we group subpopulations according to their population (see Fig. 8). Apparently, $\alpha_0 = 1.0$ denotes that there is no resource donation. The epidemic cannot spread in all the subpopulation groups for $\alpha_0 = 0.0, 0.2, 0.4$, and 0.6 [Figs. 8(a)–8(d)], respectively; whereas the epidemic breaks out in subpopulations with more population, for $\alpha_0 = 0.8$ and

1.0 [Figs. 8(e) and 8(f)]. Consequently, at the initial stage, a high donation awareness α_0 promotes the outbreak of the epidemic.

3. Effects of the parameter β

The donation willingness function in the main text [Eq. (2)] is defined with a sigmoid function. To analyze the effects of the sigmoid function on the donation willingness $q_i(t)$, we plot the function curve as shown in Fig. 9. The parameter $\eta \in [0, 1]$ controls the horizontal shift of the function, and the smaller β gets a higher initial value and increases steadily with a less slope. To interpret the role of the parameter β on the epidemic spreading, we collect the statistical properties of the network evolving with time, such as the average donation willingness $\langle q \rangle$, the average holding resources $\langle \omega \rangle$, the average infection ratio of individuals in neighboring subpopulations $\langle m \rangle$, the average infection rate $\langle \lambda \rangle$, the average recover rate $\langle \mu \rangle$, and the average effective infection rate $\langle \lambda \rangle / \langle \mu \rangle$. Under the HOD, as shown in Fig. 10, the average infection ratio of individuals in neighboring subpopulations $\langle m \rangle$ increases with time [Fig. 10(c)]. The lower β is, the faster it creases. Then subpopulations increase their average donation willingness $\langle q \rangle$ to donate resources to others [Fig. 10(a)], leading to the increasing of average infection rate $\langle \lambda \rangle$ [Fig. 10(d)]. The average holding resources $\langle \omega \rangle$ decreases with time [Fig. 10(b)], so the average recover rate $\langle \mu \rangle$ decreases [Fig. 10(e)]. Consequently, the average effective infection rate $\langle \lambda \rangle / \langle \mu \rangle$ increases with time for each β [Fig. 10(f)], and a lower β leads to a higher final $\langle \lambda \rangle / \langle \mu \rangle$. For the HED, to further interpret the

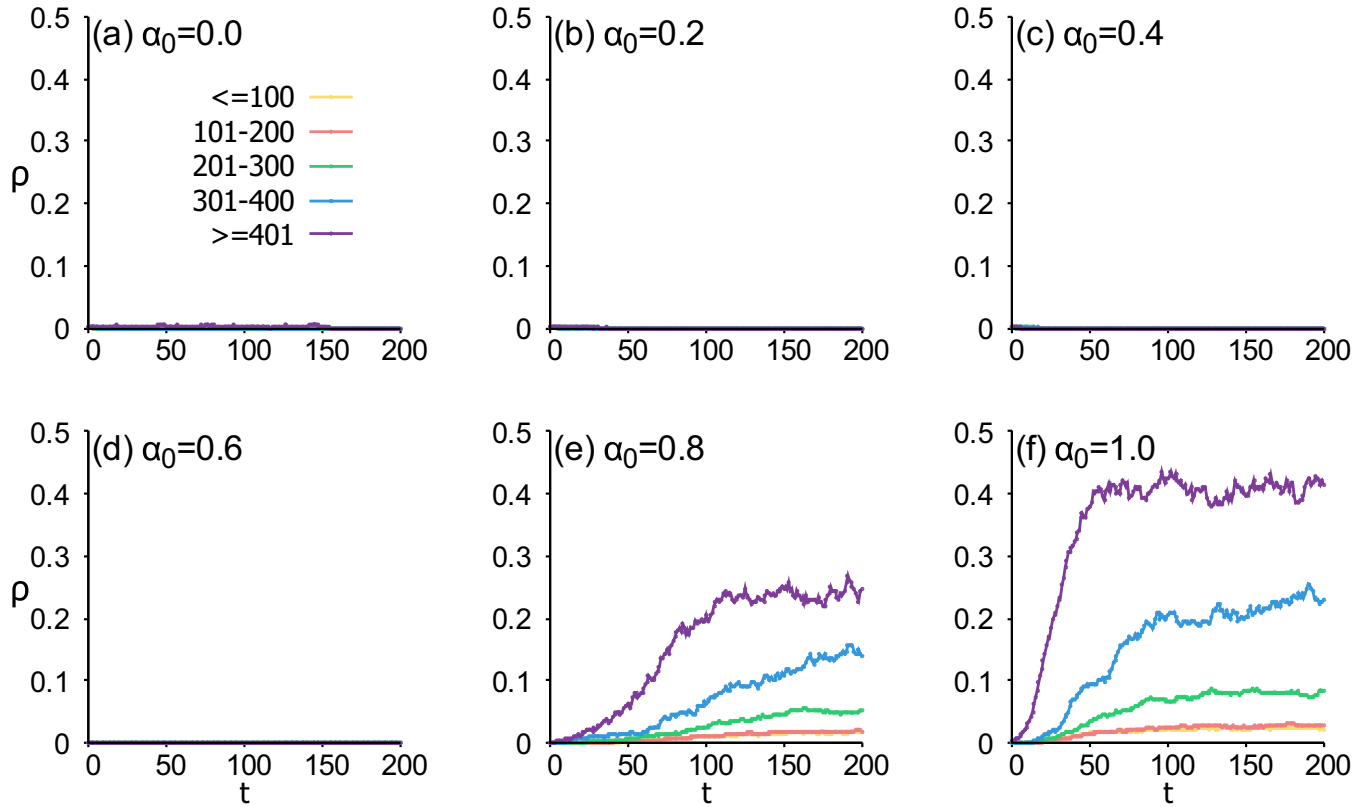


FIG. 8. The time evolution of the prevalence ρ under various values of α_0 for five subpopulation groups under the HED. The subpopulations are grouped according to their population with ≤ 100 , 101–200, 201–300, 301–400, and ≥ 401 . (a) $\alpha_0 = 0.0$, (b) $\alpha_0 = 0.2$, (c) $\alpha_0 = 0.4$, (d) $\alpha_0 = 0.6$, (e) $\alpha_0 = 0.8$, and (f) $\alpha_0 = 1.0$. The basic infection rate $\lambda = 0.0015$.

role of the donation sensitivity β near the threshold, we group subpopulations according to their population (Fig. 11). From Figs. 11(a)–11(c), the curves just present a slight fluctuation initially and finally approach to zero, which suggests that the epidemic cannot spread. From Figs. 11(d)–11(f), the curves firstly go up then approach to steadiness, and the epidemic easily diffuses especially in these subpopulations with more

population. Thus, a higher β promotes the outbreak of the epidemic especially in large-scale subpopulations.

4. Effects of the parameter θ

To explore the detailed effects of the rate of the resources' arrival θ on the epidemic spreading under the HOD, we also collect the statistical properties of the network evolving with time (Fig. 12). With time evolution, the average infection ratio of individuals in neighboring subpopulations $\langle m \rangle$ increases [Fig. 12(c)], and a higher θ leads to a lower $\langle m \rangle$. Then subpopulations increase their average donation willingness $\langle q \rangle$ to donate resources to others [Fig. 12(a)], inducing the creasing of the average infection rate $\langle \lambda \rangle$ [Fig. 12(d)]. Besides, a higher θ induces a higher average holding resources $\langle \omega \rangle$ [Fig. 12(b)] and average recover rate $\langle \mu \rangle$ [Fig. 12(e)]. Thus, according to Fig.12(f), a higher θ induces a lower final average effective infection rate $\langle \lambda \rangle / \langle \mu \rangle$.

For the HED, to further interpret the role of θ on the epidemic, we group subpopulations according to their population (Fig. 13). From Figs. 13(a)–13(d), we find that a higher θ can effectively reduce the final prevalence. However, when $\theta = 20$ or 30 [Figs. 13(e) and 13(f)], there is not evident on reducing the final epidemic prevalence. Consequently, a higher θ can decrease the final epidemic prevalence to some extent.

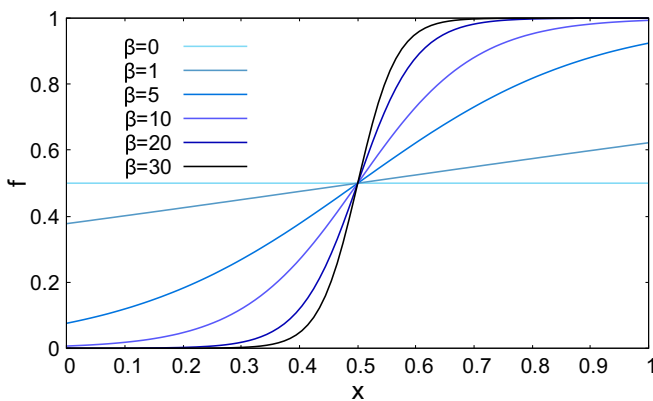


FIG. 9. The curves of the sigmoid function $f(x) = \frac{1}{1+e^{-\beta(x-\eta)}}$ for different choices of β with $\eta = 0.5$. The function become constant 0.5 when $\beta = 0$. The lower β presents a more steady growth with a higher initial function value.

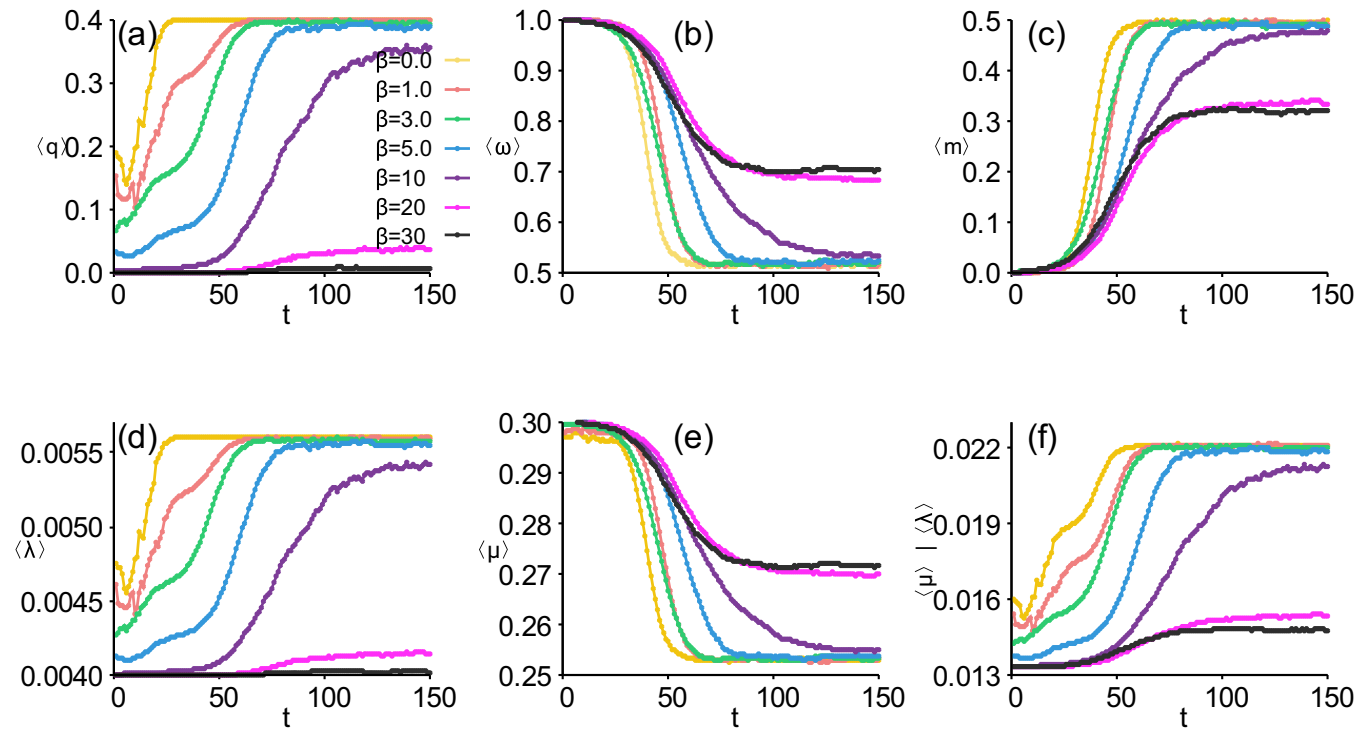


FIG. 10. The time evolution of six properties for various values of β under the HOD. (a) The average donation willingness $\langle q \rangle$; (b) the average holding resources $\langle \omega \rangle$; (c) the average infection ratio of individuals in neighboring subpopulations $\langle m \rangle$; (d) the average infection rate $\langle \lambda \rangle$; (e) the average recover rate $\langle \mu \rangle$; (f) the average effective infection rate $\langle \lambda \rangle / \langle \mu \rangle$. The basic infection rate $\lambda = 0.004$.

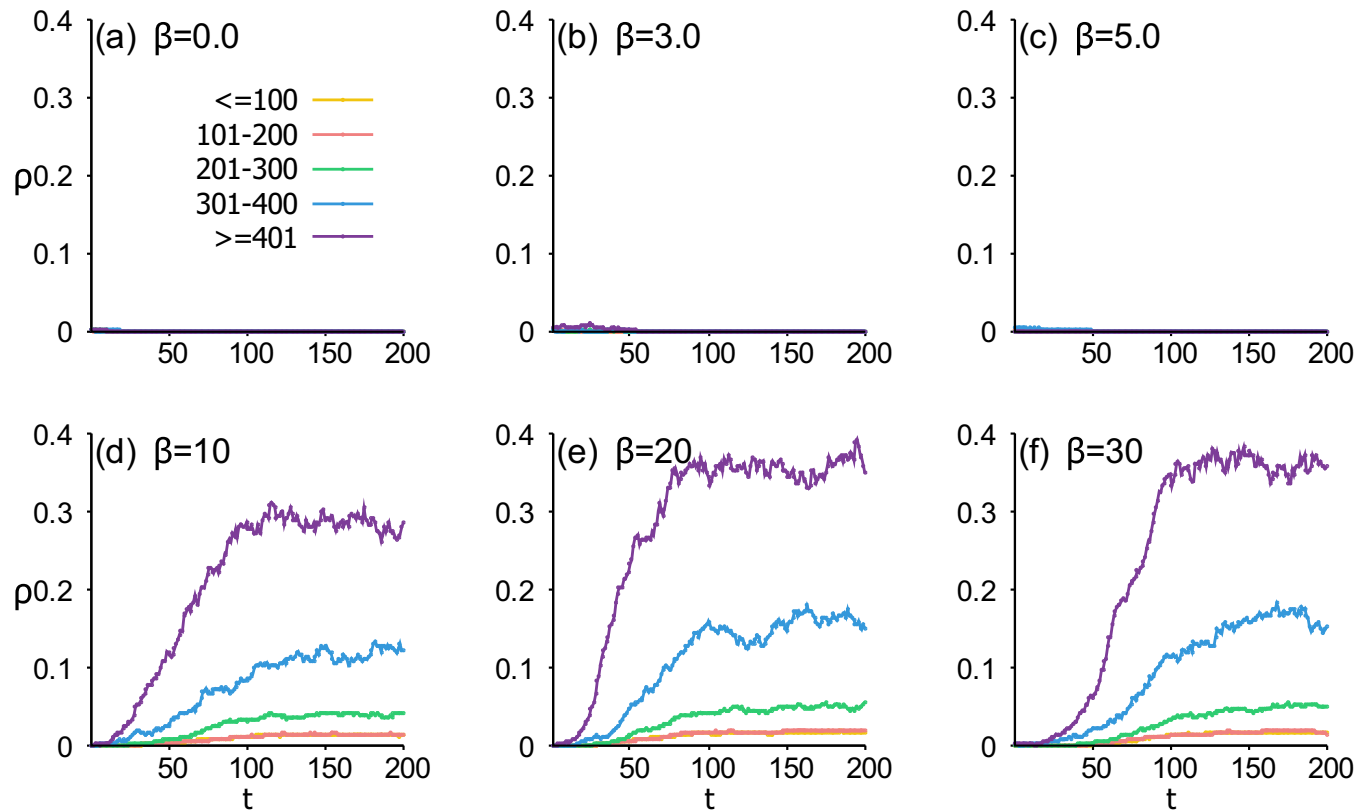


FIG. 11. The time evolution of the prevalence ρ under various values of β for five subpopulation groups under the HED. The subpopulations are grouped according to their population with ≤ 100 , $101-200$, $201-300$, $301-400$, and ≥ 401 . (a) $\beta = 0.0$, (b) $\beta = 3.0$, (c) $\beta = 5.0$, (d) $\beta = 10$, (e) $\beta = 20$, and (f) $\beta = 30$. The basic infection rate $\lambda = 0.0015$.

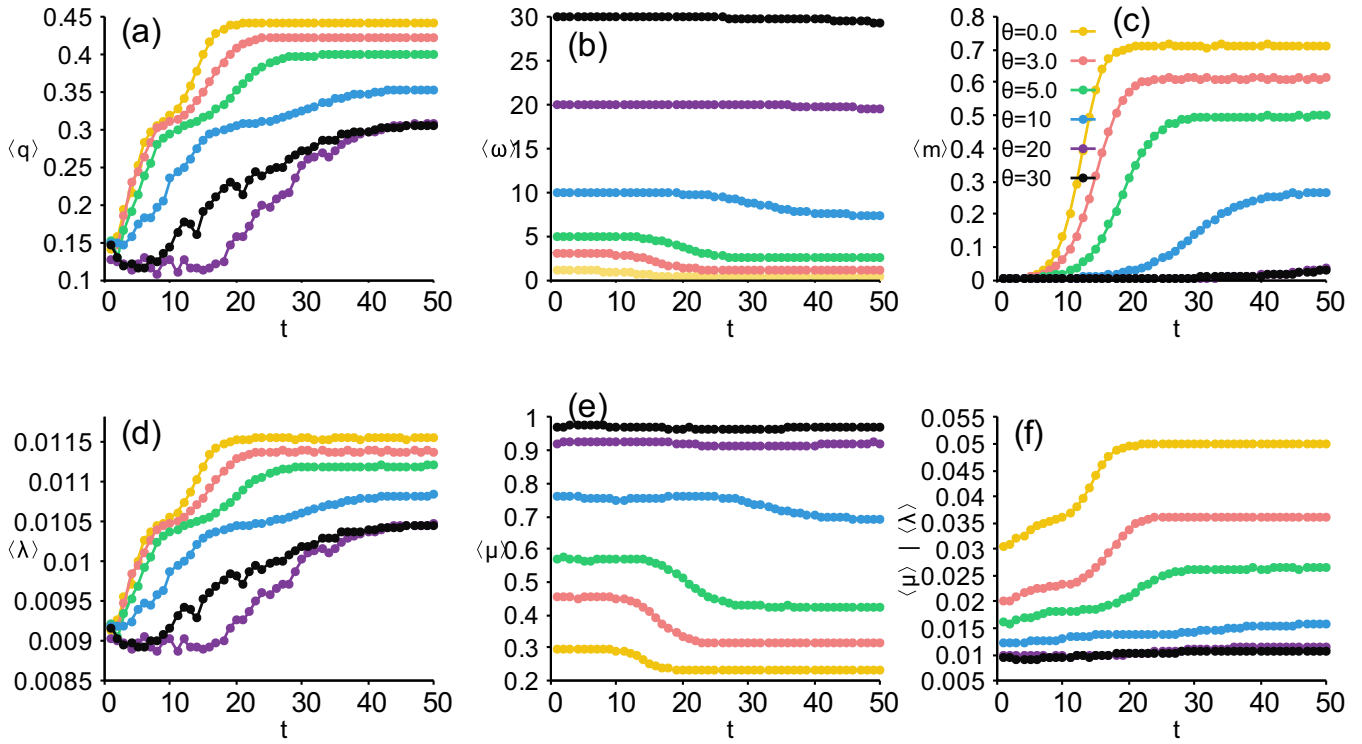


FIG. 12. The time evolution of six properties for various values of θ under the HOD. (a) The average donation willingness $\langle q \rangle$; (b) the average holding resources $\langle \omega \rangle$; (c) the average infection ratio of individuals in neighboring subpopulations $\langle m \rangle$; (d) the average infection rate $\langle \lambda \rangle$; (e) the average recover rate $\langle \mu \rangle$; (f) the average effective infection rate $\langle \lambda \rangle / \langle \mu \rangle$. The basic infection rate $\lambda = 0.01$.

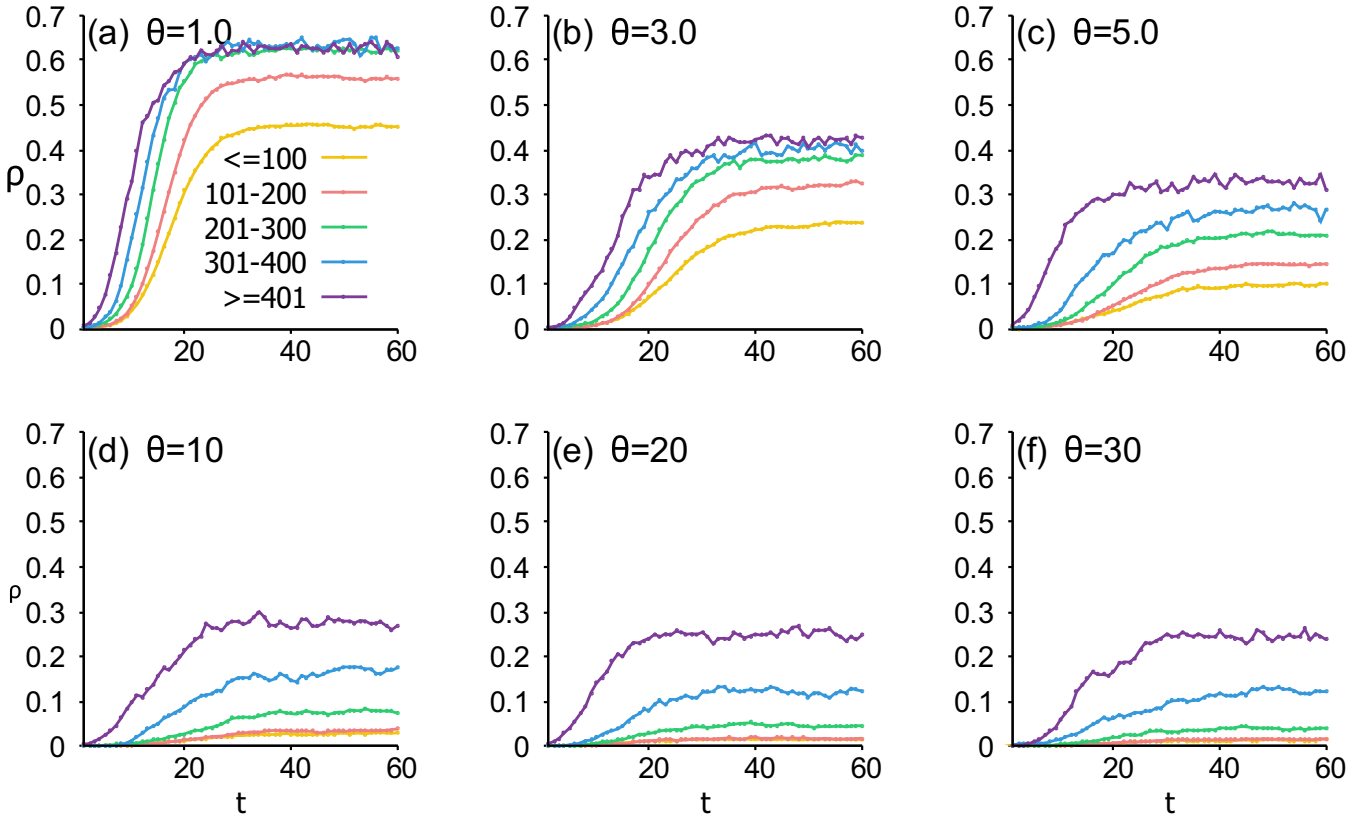


FIG. 13. The time evolution of the prevalence ρ under various values of θ for five subpopulation groups. The subpopulations are grouped according to their population with ≤ 100 , 101–200, 201–300, 301–400, and ≥ 401 . (a) $\theta = 1.0$, (b) $\theta = 3.0$, (c) $\theta = 5.0$, (d) $\theta = 10$, (e) $\theta = 20$, and (f) $\theta = 30$. The basic infection rate $\lambda = 0.01$.

- [1] A. Abbott, China and Germany join forces over SARS, *Nature (London)* **423**, 791 (2003).
- [2] D. Cyranoski, WHO issues rallying cry to keep fight against SARS on track, *Nature (London)* **423**, 905 (2003).
- [3] N. S. Zhong, B. J. Zheng, Y. M. Li, L. L. M. Poon, Z. H. Xie, K. H. Chan, P. H. Li, S. Y. Tan, Q. Chang, J. P. Xie, X. Q. Liu, J. Xu, D. X. Li, K. Y. Yuen, J. S. M. Peiris, and Y. Guan, Epidemiology and cause of severe acute respiratory syndrome (SARS) in Guangdong, People's Republic of China, in February, 2003, *Lancet* **362**, 1353 (2003).
- [4] R. Q. Liu, J. L. Wang, Y. Shao, X. J. Wang, H. L. Zhang, L. Shuai, J. Y. Ge, Z. Y. Wen, and Z. G. Bu, A recombinant VSV-vectored MERS-CoV vaccine induces neutralizing antibody and T cell responses in rhesus monkeys after single dose immunization, *Antiviral Res.* **150**, 30 (2018).
- [5] A. S. Omrani, J. A. Al-Tawfiq, and Z. A. Memish, Middle East respiratory syndrome coronavirus (MERS-CoV): Animal to human interaction, *Pathog. Glob. Health* **109**, 354 (2015).
- [6] X. Qiu, G. Wong, J. Audet, A. Bello, L. Fernando, J. B. Alimonti, H. Fausther-Bovendo, H. Wei, J. Aviles, E. Hiatt, A. Johnson, J. Morton, K. Swope, O. Bohorov, N. Bohorova, C. Goodman, D. Kim, M. H. Pauly, J. Velasco, J. Pettitt *et al.*, Reversion of advanced Ebola virus disease in nonhuman primates with ZMapp, *Nature (London)* **514**, 47 (2014).
- [7] S. K. Gire, A. Goba, K. G. Andersen, R. S. Sealfon, D. J. Park, L. Kanneh, S. Jalloh, M. Momoh, and Fullah, Genomic surveillance elucidates Ebola virus origin and transmission during the 2014 outbreak, *Science* **345**, 1369 (2014).
- [8] S. R. Meakin, M. J. Tildesley, E. Davis, and M. J. Keeling, A metapopulation model for the 2018 Ebola virus disease outbreak in Equateur province in the Democratic Republic of the Congo, *Am. J. Trop. Med. Hyg.* **101**, 467 (2019).
- [9] M. Chinazzi, J. T. Davis, M. Ajelli, C. Gioannini, M. Litvinova, S. Merler, Y. Piontti, A. Pastore, K. Mu, L. Rossi, K. Sun, C. Viboud, X. Xiong, H. Yu, M. E. Halloran, J. Longini, I. M. Longini, and A. Vespignani, The effect of travel restrictions on the spread of the 2019 novel coronavirus (COVID-19) outbreak, *Science* **368**, 395 (2020).
- [10] C. Y. Wang, R. Y. Pan, X. Y. Wan, Y. L. Tan, L. K. Xu, C. S. Ho, and R. C. Ho, Immediate psychological responses and associated factors during the initial stage of the 2019 coronavirus disease (COVID-19) epidemic among the general population in China, *Int. J. Environ. Res. Public Health* **17**, 1729 (2020).
- [11] M. L. Wang, R. Y. Cao, L. K. Zhang, X. L. Yang, J. Liu, M. Y. Xu, Z. L. Shi, Z. H. Hu, W. Zhong, and G. F. Xiao, Remdesivir and chloroquine effectively inhibit the recently emerged novel coronavirus (2019-nCoV) *in vitro*, *Cell Res.* **30**, 269 (2020).
- [12] WHO, WHO Coronavirus Disease (COVID-19) Dashboard, Report (2021), <https://covid19.who.int>.
- [13] M. L. Ranney, V. Griffith, and A. K. Jha, Critical supply shortages—The need for ventilators and personal protective equipment during the Covid-19 pandemic, *N. Engl. J. Med.* **382**, e41 (2020).
- [14] S. Feng, C. Shen, N. Xia, W. Song, M. Z. Fan, and B. J. Cowling, Rational use of face masks in the COVID-19 pandemic, *Lancet. Resp. Med.* **8**, 434 (2020).
- [15] A. Odone, D. Delmonte, T. Scognamiglio, and C. Signorelli, COVID-19 deaths in Lombardy, Italy: Data in context, *Lancet Public Health* **5**, e310 (2020).
- [16] D. Helbing, Globally networked risks and how to respond, *Nature (London)* **497**, 51 (2013).
- [17] A. Majdandzic, B. Podobnik, S. V. Buldyrev, D. Y. Kenett, S. Havlin, and H. E. Stanley, Spontaneous recovery in dynamical networks, *Nat. Phys.* **10**, 34 (2014).
- [18] L. Bottcher, O. Woolley-Meza, N. A. Araujo, H. J. Herrmann, and D. Helbing, Disease-induced resource constraints can trigger explosive epidemics, *Sci. Rep.* **5**, 16571 (2015).
- [19] V. Colizza, A. Barrat, M. Barthelemy, A. J. Valleron, and A. Vespignani, Modeling the worldwide spread of pandemic influenza: Baseline case and containment interventions, *PLoS Med.* **4**, e13 (2007).
- [20] L. Bottcher, O. Woolley-Meza, E. Goles, D. Helbing, and H. J. Herrmann, Connectivity disruption sparks explosive epidemic spreading, *Phys. Rev. E* **93**, 042315 (2016).
- [21] C. J. Worby and H. H. Chang, Face mask use in the general population and optimal resource allocation during the covid-19 pandemic, *Nat. Commun.* **11**, 4049 (2020).
- [22] H. Chen, G. Li, H. Zhang, and Z. Hou, Optimal allocation of resources for suppressing epidemic spreading on networks, *Phys. Rev. E* **96**, 012321 (2017).
- [23] X. L. Chen, Q. H. Liu, R. J. Wang, Q. Li, and W. Wang, Self-awareness-based resource allocation strategy for containment of epidemic spreading, *Complexity* **2020**, 3256415 (2020).
- [24] X. L. Chen, R. J. Wang, M. Tang, S. M. Cai, H. E. Stanley, and L. A. Braunstein, Suppressing epidemic spreading in multiplex networks with social-support, *New J. Phys.* **20**, 013007 (2018).
- [25] X. L. Chen, W. Wang, S. M. Cai, H. E. Stanley, and L. A. Braunstein, Optimal resource diffusion for suppressing disease spreading in multiplex networks, *J. Stat. Mech.* (2018) 053501.
- [26] X. C. Wang, X. Z. Zhu, X. F. Tao, J. H. Xiao, W. Wang, and Y. C. Lai, Anomalous role of information diffusion in epidemic spreading, *Phys. Rev. Research* **3**, 013157 (2021).
- [27] J. Jiang and T. Zhou, Resource control of epidemic spreading through a multilayer network, *Sci. Rep.* **8**, 1629 (2018).
- [28] D. Soriano-Panos, L. Lotero, A. Arenas, and J. Gomez-Gardenes, Spreading Processes in Multiplex Metapopulations Containing Different Mobility Networks, *Phys. Rev. X* **8**, 031039 (2018).
- [29] A. Apolloni, C. Poletto, J. J. Ramasco, P. Jensen, and V. Colizza, Metapopulation epidemic models with heterogeneous mixing and travel behaviour, *Theor. Biol. Med. Model.* **11**, 3 (2014).
- [30] C. Shen, H. Chen, and Z. Hou, Strategy to suppress epidemic explosion in heterogeneous metapopulation networks, *Phys. Rev. E* **86**, 036114 (2012).
- [31] D. Balcan and A. Vespignani, Phase transitions in contagion processes mediated by recurrent mobility patterns, *Nat. Phys.* **7**, 581 (2011).
- [32] V. Colizza and A. Vespignani, Epidemic modeling in metapopulation systems with heterogeneous coupling pattern: Theory and simulations, *J. Theor. Biol.* **251**, 450 (2008).
- [33] N. Perra, Nonpharmaceutical interventions during the COVID-19 pandemic: A review, *Phys. Rep.* **913**, 1 (2021).
- [34] V. Colizza, R. Pastor-Satorras, and A. Vespignani, Reaction-diffusion processes and metapopulation models in heterogeneous networks, *Nat. Phys.* **3**, 276 (2007).

- [35] J. T. Davis, N. Perra, Q. Zhang, Y. Moreno, and A. Vespignani, Phase transitions in information spreading on structured populations, *Nat. Phys.* **16**, 590 (2020).
- [36] J. Gómez-Gardeñes, D. Soriano-Paños, and A. Arenas, Critical regimes driven by recurrent mobility patterns of reaction–diffusion processes in networks, *Nat. Phys.* **14**, 391 (2018).
- [37] B. Wang, M. Gou, Y. K. Guo, G. Tanaka, and Y. X. Han, Network structure-based interventions on spatial spread of epidemics in metapopulation networks, *Phys. Rev. E* **102**, 062306 (2020).
- [38] N. Bailey, The mathematical theory of infectious diseases and its applications, *J. Oper. Res. Soc.* **28**, 479 (1977).
- [39] X. Z. Zhu, Y. X. Liu, S. F. Wang, R. J. Wang, X. L. Chen, and W. Wang, Allocating resources for epidemic spreading on metapopulation networks, *Appl. Math. Comput.* **411**, 126531 (2021).